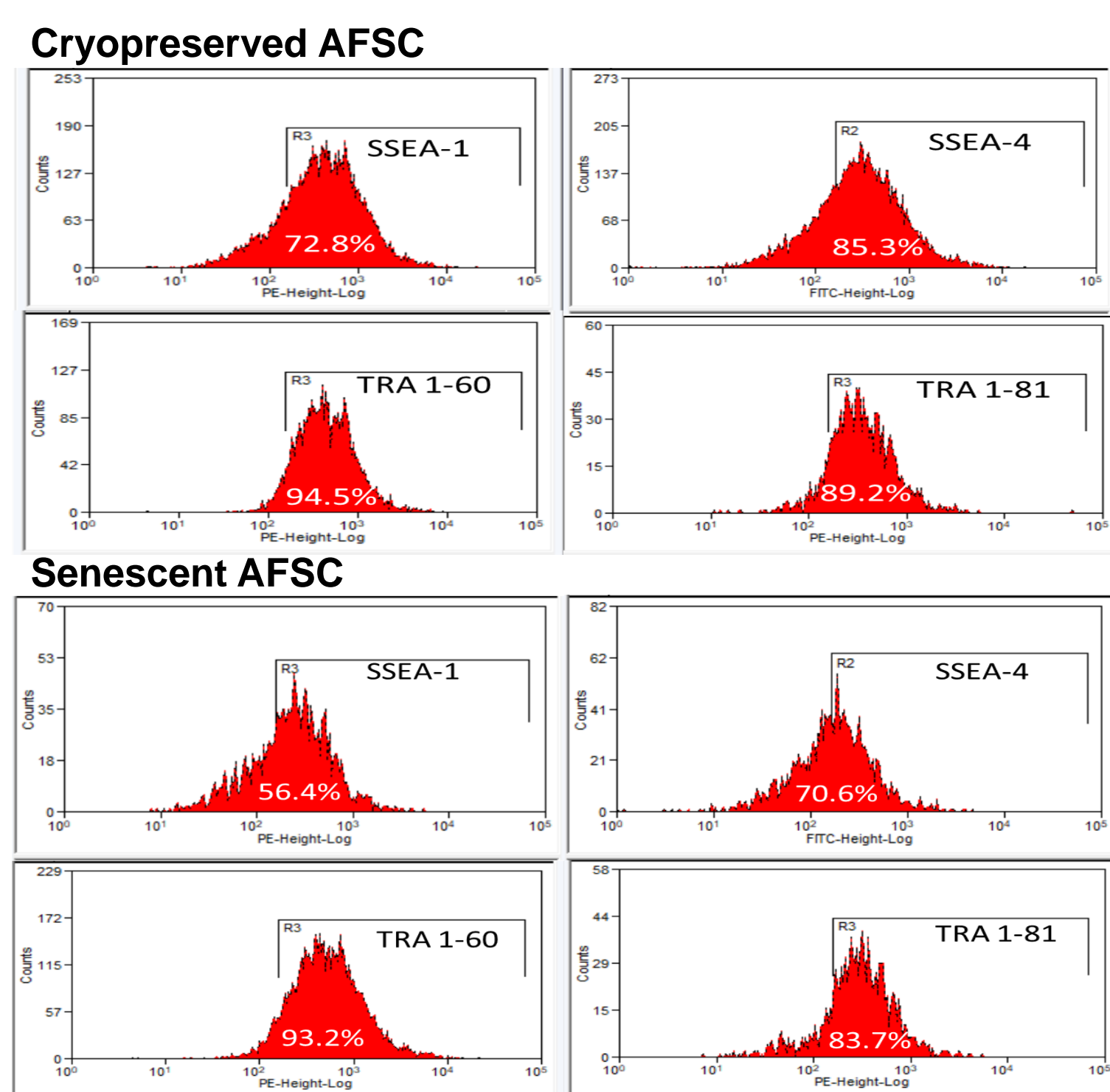


**Introduction** Senescence represents an adaptive cellular response to potential stress. Although to date there is no unique marker to distinguish senescent cells from non-proliferating ones, a combination of markers can lead us to a senescent phenotype called senescence-associated secretory phenotype (SASP), consisting in a number of metabolic changes that try to remove stress factors. The present study aims to explore activation of specific signaling molecules associated with SASP in our in vitro senescence model.

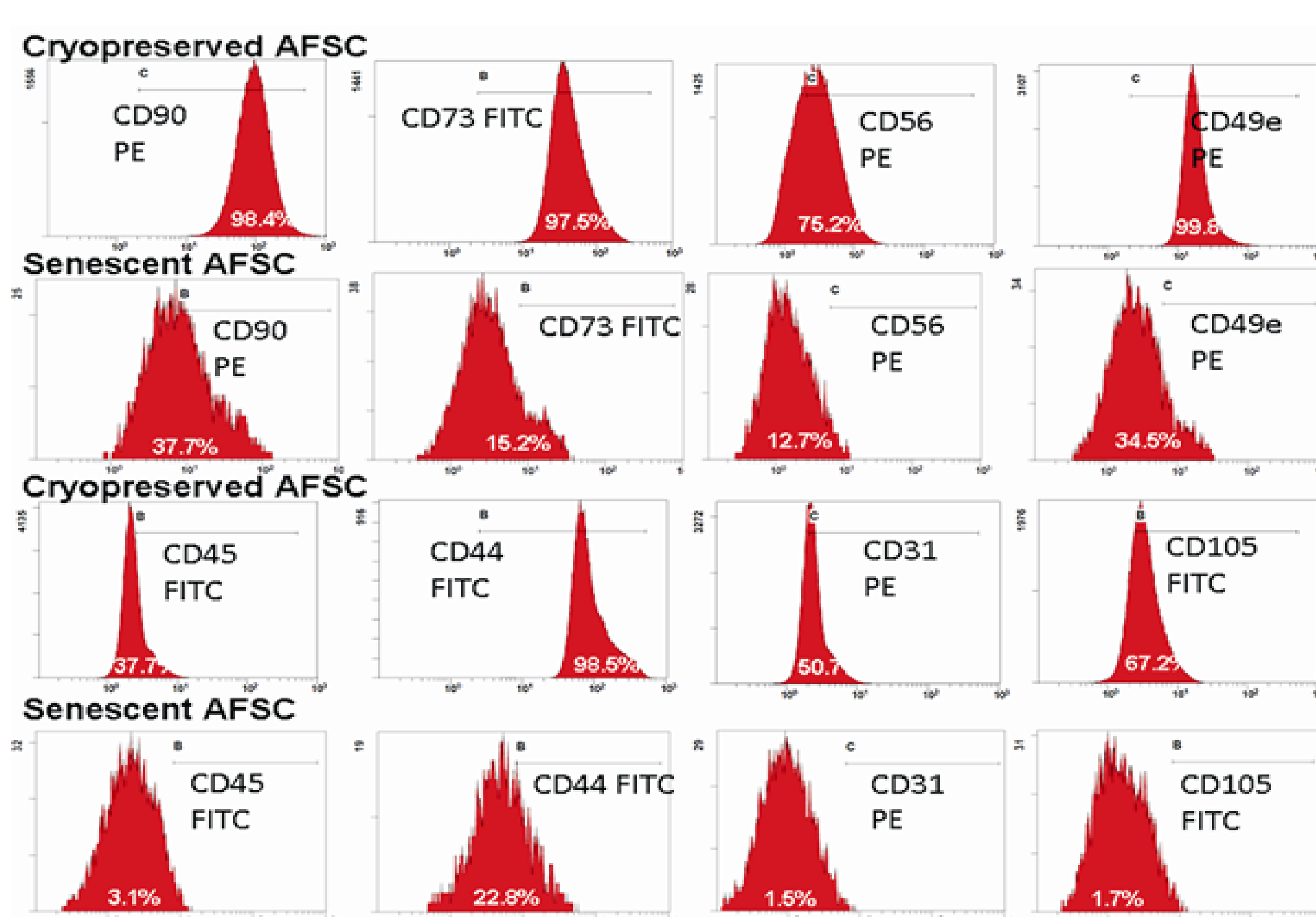
## Materials and methods

Human amniotic fluid stem cells (AFSC) at passages 2 or 3 and senescent cells (maintained 40 days in culture without any passage) were analyzed for modification of stem cell markers by flow cytometry, for inflammatory markers by qRT-PCR and for ion currents by patch-clamp.

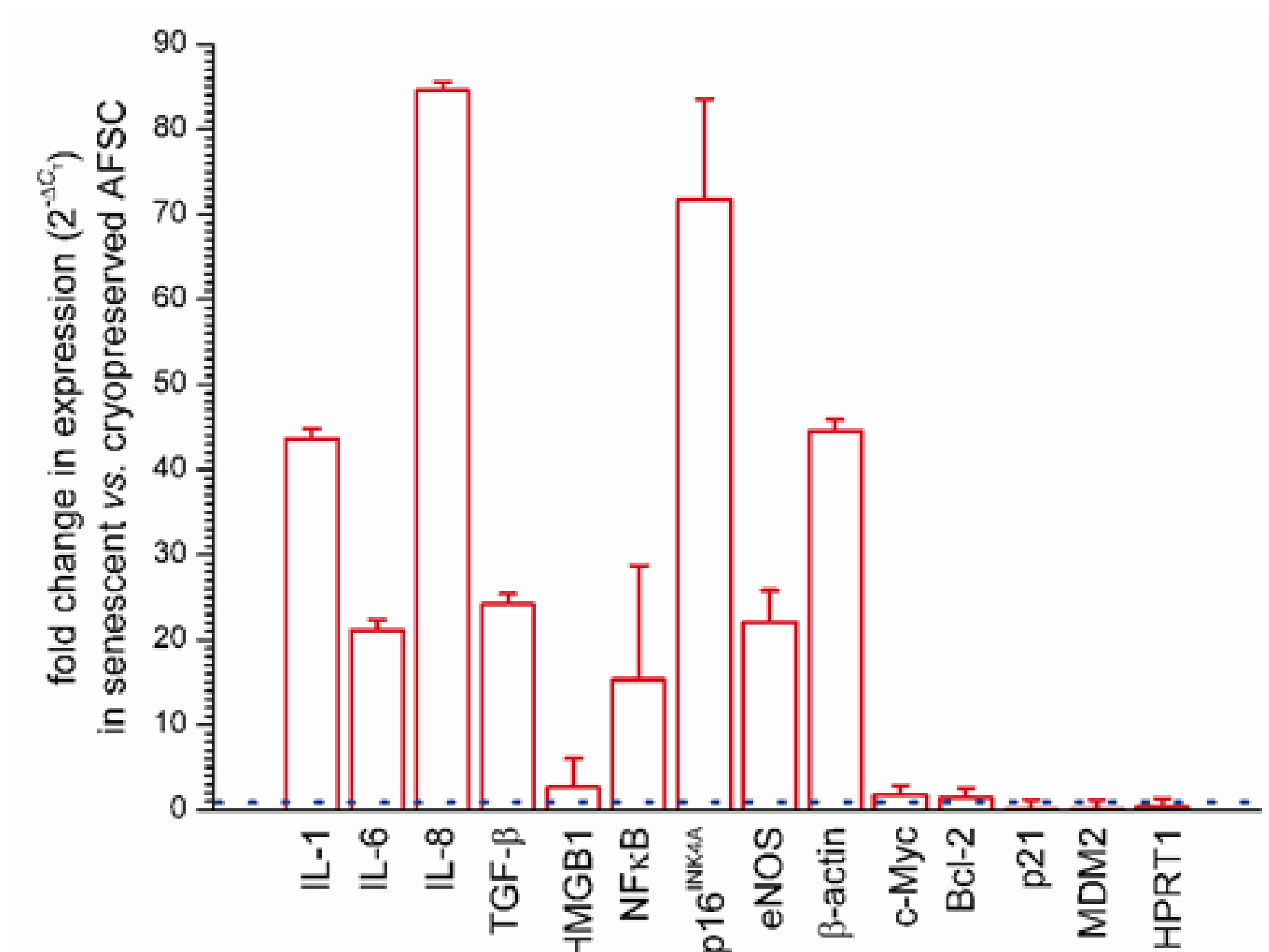
## Results and Discussions



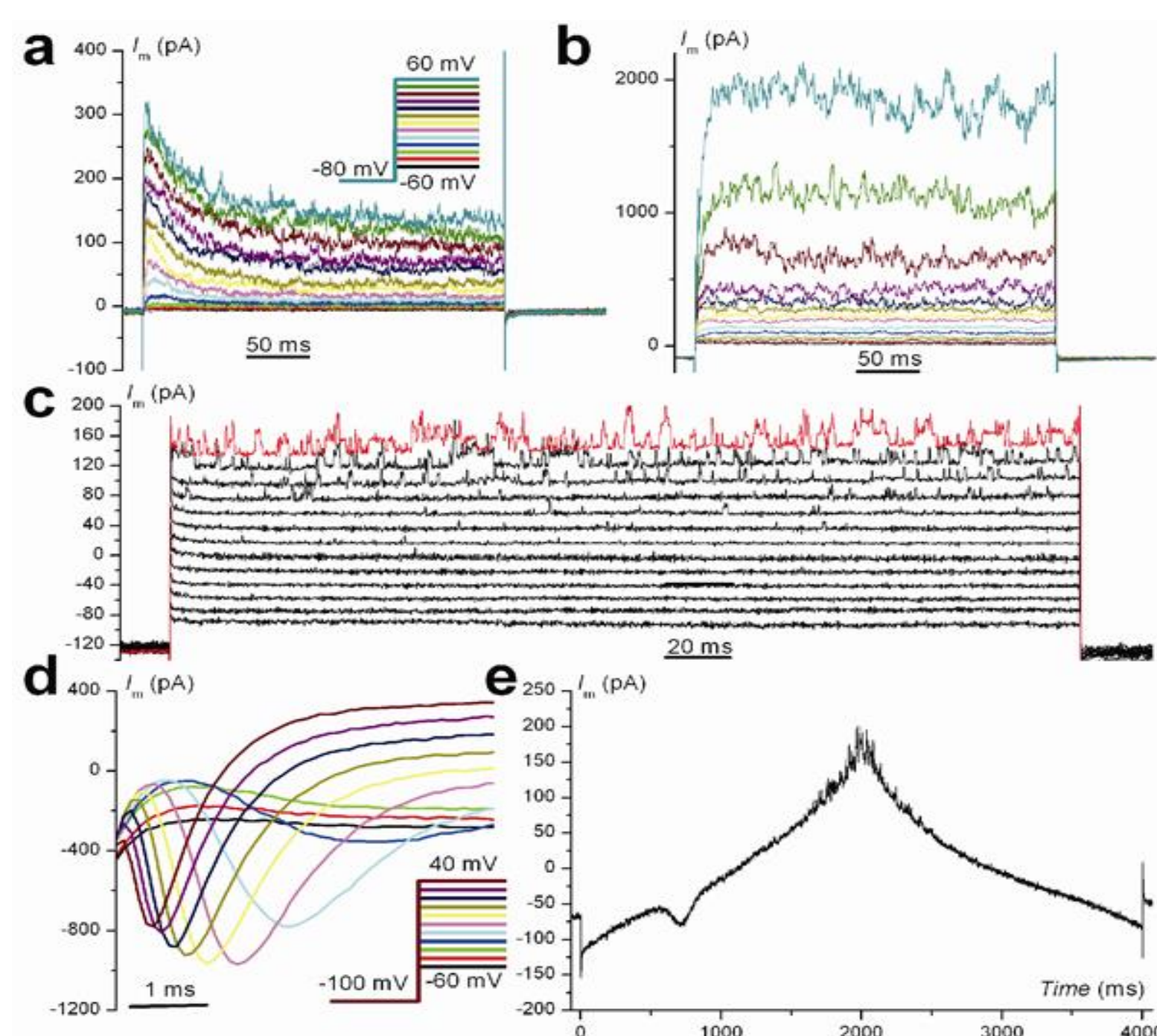
Flow cytometry assays for pluripotency stem cell markers SSEA-1, SSEA-4, TRA1-60, TRA1-81 in cryopreserved and senescent AFSC. Percentages of positive cells for each marker indicated that the senescent cells did not lose pluripotency.



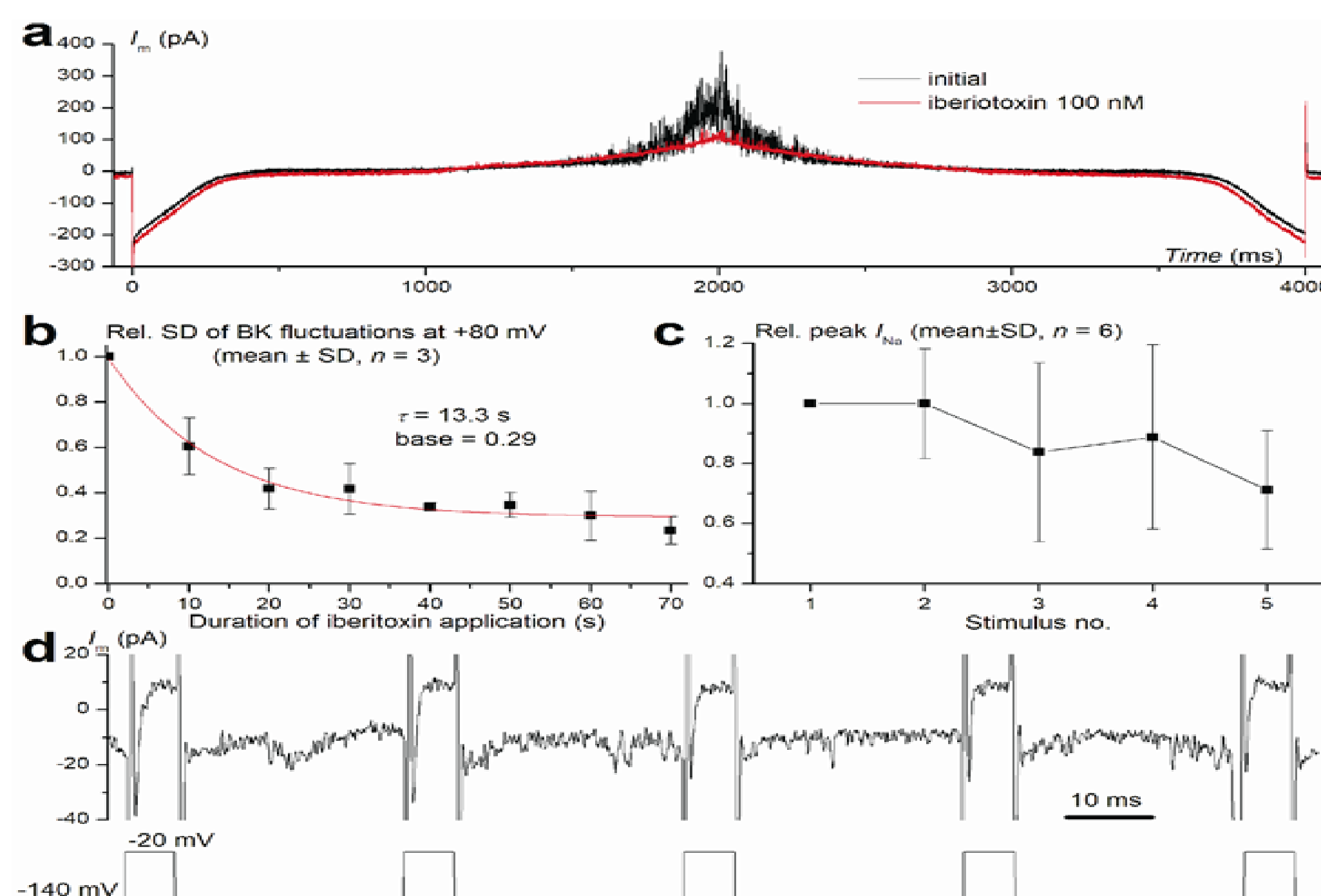
Flow cytometry assays for mesenchymal stem cell markers CD31, CD44, CD45, CD49e, CD56, CD73, CD90, CD105 in cryopreserved and senescent AFSC. Percentages of positive cells for each marker are indicated on the corresponding distribution histograms.



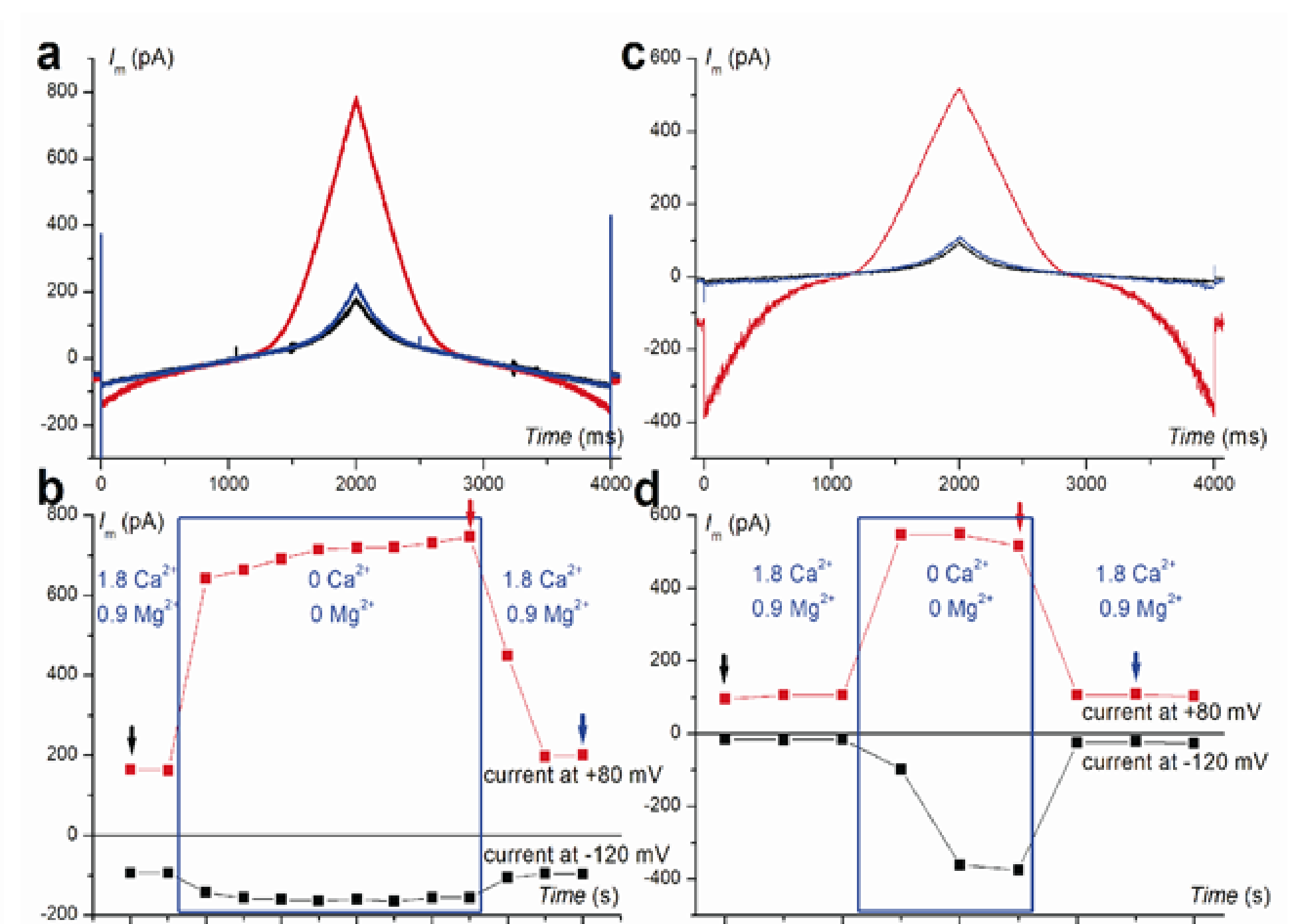
Differences in gene expression levels between senescent and early passages (cryopreserved) AFSC. The fold-change in expression in senescent vs. cryopreserved AFSC was computed as  $2^{-\Delta C_t}$ .



Ion currents recorded in AFSC. a and b. Two voltage-clamp recordings in senescent AFSC via automated patch-clamp, using a general protocol for K<sup>+</sup> currents. I<sub>or</sub> and BK fluctuations are visible in both recordings, while I<sub>A</sub> can be noticed only in a; c. Same protocol applied to a cryopreserved AFSC with very small current levels; single-channel BK openings can be noticed at larger depolarizations (+20 to +60 mV); d. Voltage-dependent Na<sup>+</sup> current (I<sub>Na</sub>) in a senescent AFSC. e. Double-ramp voltage-clamp protocol applied to a senescent AFSC; a small T-type Ca<sup>2+</sup> channel-like current with a threshold of ~-50 mV is present on the ascending ramp.



Pharmacology assays in cryopreserved AFSC via automated patch-clamp. a. Double-ramp voltage-clamp protocol with traces recorded before and after application of iberitoxin 100 nM that blocked BK current fluctuations at positive potentials; b. Kinetics of BK channels block by iberitoxin: Fitting with a mono-exponential function yielded a time constant  $\tau = 13.3$  s and a base of 0.29; c. Kinetics of use-dependent I<sub>Na</sub> block by lidocaine 200  $\mu$ M (relative peak I<sub>Na</sub> amplitudes for 5 consecutive depolarizing pulses, mean  $\pm$  SD of n=3 experiments); d. Voltage-clamp protocol for study of use-dependent I<sub>Na</sub> block by lidocaine (only the first 5 of 40 consecutive pulses are shown).



TRPM7-like currents in AFSC. a. and c. Current traces recorded with the double-ramp voltage protocol in a cryopreserved AFSC (a.) and a senescent AFSC (c.) before, during, and after divalent cation removal from external solutions (timing is marked with arrows of appropriate color in b. and d., respectively), revealing a large reversible monovalent cation current with a peculiar I-V plot compatible with TRPM7; b. and d. Time course of current amplitudes at -120 mV and +80 mV during external cation removal in the experiments shown in a. and c.

**Conclusion.** In our model we evidenced specific changes in senescent vs. early passages AFSC, suggesting a shift from an anti-inflammatory phenotype to a proinflammatory one, thus limiting their therapeutic potential.

**Acknowledgments.** The work was supported by project nr. 19/2018, PN-III-P1-1.1-PD-2016-1660 financed by the Executive Agency for Higher Education, Research, Development and Innovation Funding (UEFISCDI).